

Rethinking the Role of the Middle Longitudinal Fascicle in Language and Auditory Pathways

Yibao Wang¹, Juan C. Fernández-Miranda¹, Timothy Verstynen², Sudhir Pathak², Walter Schneider² and Fang-Cheng Yeh³

¹Department of Neurological Surgery, University of Pittsburgh Medical Center, Pittsburgh, PA 15213, USA, ²Learning Research and Development Center, University of Pittsburgh, Pittsburgh, PA 15213, USA and ³Department of Biomedical Engineering, Carnegie Mellon University, Pittsburgh, PA 15213, USA

Address correspondence to: Juan C. Fernández-Miranda, 200 Lothrop St, Suite B-400, Department of Neurological Surgery, University of Pittsburgh Medical Center, Pittsburgh, PA 15213, USA. Email: fernandezmirandajc@upmc.edu

The middle longitudinal fascicle (MdLF) was originally described in the monkey brain as a pathway that interconnects the superior temporal and angular gyri. Only recently have diffusion tensor imaging studies provided some evidence of its existence in humans, with a connectivity pattern similar to that in monkeys and a potential role in the language system. In this study, we combine high-angular-resolution fiber tractography and fiber microdissection techniques to determine the trajectory, cortical connectivity, and a quantitative analysis of the MdLF. Here, we analyze diffusion spectrum imaging (DSI) studies in 6 subjects (subject-specific approach) and in a template of 90 DSI studies (NTU-90 Atlas). Our tractography and microdissection results show that the human MdLF differs significantly from the monkey. Indeed, the human MdLF interconnects the superior temporal gyrus with the superior parietal lobule and parietooccipital region, and has only minor connections with the angular gyrus. On the basis of the roles of these interconnected cortical regions, we hypothesize that, rather than a language-related tract, the MdLF may contribute to the dorsal "where" pathway of the auditory system.

Keywords: auditory system, fiber tractography, language, middle longitudinal fasscile, white matter

Introduction

The middle longitudinal fascicle (MdLF) was described many years ago as a pathway that interconnects temporal and parietal regions in the rhesus monkey (Seltzer and Pandya 1984). Specifically, this fiber bundle emerges from the caudal inferior parietal lobule and courses in the white matter of the superior temporal gyrus (Schmahmann and Pandya 2006). Based on its location and cortical connectivity, the MdLF may play a significant role in human higher cortical functions such as language and attention (Schmahmann and Pandya 2006). With evolution, however, the temporal and parietal regions of the human brain are significantly different from their monkey counterparts, so extrapolating results from monkey studies to humans could be misleading (Rilling et al. 2008).

Classical neuroanatomical studies of the white matter of the human brain, despite defining most of today's known major fiber tracts (such as the superior and inferior longitudinal fascicles), did not describe the existence of the MdLF (Ludwig and Klingler 1956; Schmahmann and Pandya 2006). Contemporary fiber microdissection studies on human white matter have also failed to demonstrate the presence of the MdLF (Türe et al. 2000; Fernández-Miranda, Rhoton, Kakizawa et al. 2008). In recent years, the application of magnetic resonance (MR)-based fiber-tracking techniques, such as diffusion tensor imaging (DTI), has revitalized the study of the complex

anatomy of the white matter of the human brain, and has provided some evidence of the existence of the MdLF in the human brain (Makris et al. 2009). DTI, however, is unable to determine with accuracy the origin and destination of fibers (Alexander and Barker 2005; Schmahmann and Pandya 2006) and cannot directly image multiple fiber orientations within a single voxel (Wedeen et al. 2008).

In this study, we investigate the connectivity structure of the human MdLF using a high-resolution form of white matter tractography that can sufficiently resolve complex fiber crossings such as those that affect the MdLF. The tractography studies are performed using both a subject-specific approach and a template approach. We complement this analysis with focused fiber microdissection studies of the MdLF in human brains to confirm the underlying neuroanatomy. The results of this study present a novel and detailed account of the neuroanatomy of the MdLF, with a distinct connectivity pattern that may help to understand better the functional role of this fiber bundle in the human brain.

Methods

High-Angular-Resolution Fiber Tractography Technique

Participants

Six neurologically healthy adults (5 males; all right handed; age range: 22–31 years) from the local University of Pittsburgh community took part in this experiment, conducted as part of a larger data collection effort associated with the 2009 Pittsburgh Brain Competition. All participants were prescreened prior to scanning to rule out any contraindications to MR imaging. The internal review board at the University of Pittsburgh approved all the procedures used here and written consent was obtained from all participants prior to testing.

Image Acquisition and Reconstruction

DSI data were acquired on 3T Tim Trio System (Siemens) using a 32-channel coil. This involved a 43-min, 257-direction scan using a twice-refocused spin-echo echo-planar imaging sequence and multiple q values [repetition time (TR)=9.916 ms, echo time (TE)=157 ms, voxel size=2.4 × 2.4 × 2.4 mm, field of view (FoV)=231 × 231 mm, $b_{\max}=7000 \text{ s/mm}^2$]. For anatomical comparisons, we also included the high-resolution anatomical imaging, employing a 9-min T_1 -weighted axial magnetization prepared rapid gradient echo (MPRAGE) sequence (TR=2110 ms, TE=2.63 ms, flip angle=8°, 176 slices, FoV=256 × 256 mm², voxel size=0.5 × 0.5 × 1.0 mm³). DSI data were reconstructed using a generalized Q-sampling imaging approach (Yeh et al. 2010). The orientation distribution functions (ODFs) were reconstructed to 362 discrete sampling directions and a mean diffusion distance of 1.2.

DSI Template

In addition to subject-specific analysis, we also conduct fiber tracking on a publicly available DSI template. The DSI template is the NTU-90

atlas (Yeh and Tseng 2011), which includes 45 males and 45 female subjects. The age of the 90 subjects ranged from 18 to 60 years, and the mean ages of the male and female subjects were 32.58 and 33.58 years. The spatial resolution of the template is 2 mm. The template is the average of the normalized subject data in the ICBM-152 space (a standard space introduced by the International Consortium for Brain Mapping). The white matter surface is rendered independently from an externally supplied $1 \times 1 \times 1$ -mm resolution ICBM-152 white matter image (Fonov et al. 2011). The NTU-90 atlas is available free for download at dsi-studio.labsolver.org.

Fiber Tracking and Analysis

For the fiber-tracking datasets, all fiber tracking was performed using DSI Studio (<http://dsi-studio.labsolver.org>). Rather than adopt a whole-brain fiber-tracking procedure, we chose to use an ODF-streamlined region of interest (ROI)-based approach (Yeh et al. 2010). Tracks were generated using an ODF-streamline version of the FACT algorithm (Basser et al. 2000; Yeh et al. 2010). Using a random-seeding approach, we initiated tracking, from each random position within the seed mask, in the direction of the most prominent fiber. In voxels with multiple fiber orientations, fiber tracking was initiated separately for each orientation, and fiber progression continued with a step size of 1.2 mm, minimum fiber length of 20 mm, and turning angle threshold of 60°. If multiple fiber orientations exist in the current progression location, the fiber orientation that is nearest to the incoming direction and forms a turning angle smaller than 60° is selected to determine the next moving direction. To smooth each track, the next moving directional estimate of each voxel was weighted by 20% of the previous incoming direction and 80% of the nearest fiber orientation. This progression was repeated until the quantitative anisotropy (QA) (Yeh et al. 2010) of the fiber orientation dropped below a preset threshold (0.03–0.06 depending on the subject) or there was no fiber selected within the 60° angular range in the progression. The QA termination threshold was adjusted on a per subject basis depending on the relative signal to noise of each scan. Once tracked, all streamlines were saved in the TrackVis file format. As the smoothing parameter may affect the tracking result, and the optimal value can be different for different tracking targets, we conducted a preliminary study to determine the smoothing parameter used in our study, which is described in the following. We fixed other tracking parameters and used the same regions of interests in fiber tracking (as stated previously). Different smoothing parameters (80%, 60%, 40%, 20%, and no smoothing) were applied to generate 10 000 fiber tracks for each parameter. The qualitative comparison was conducted by inspecting the fiber trajectories, and the optimal parameter was selected by the results that offered the tractography with less false fibers, including premature termination, false turning, and false connection.

For the MdLF, a ROI mask was drawn on each single axial slice along the superior temporal gyrus to serve as seed region for the fiber-tracking algorithm (Fig. 1A). A second ROI mask on the coronal plane along the precentral region is used to exclude the arcuate fascicle fibers that pass from the posterior part of superior temporal gyrus to the prefrontal region. Segmentation of the MdLF was performed using TrackVis software. To analyze the spatial relationship of the MdLF with adjacent association tracts, we perform fiber reconstruction of the arcuate, inferior frontooccipital, and inferior longitudinal fascicles. For the arcuate fascicle, we used two different ROIs: one along the posterior temporal region and another at the posterior frontal region (Fernández-Miranda, Rhoton, Kakizawa et al. 2008). For the inferior frontooccipital fasciculus, we employed seeds around the ventral part of the external capsule (Fernández-Miranda, Rhoton, Alvarez-Linera et al. 2008; Fernández-Miranda, Rhoton, Kakizawa et al. 2008). For the inferior longitudinal fascicle, we used two different ROIs: one along the anterior temporal region and another at the occipital region (Fernández-Miranda, Rhoton, Kakizawa et al. 2008). The fiber tracking parameters were the same as those used for the reconstruction of the MdLF.

Cytoarchitectonic and Anatomical Segmentation

Cortical parcellation was performed using two methods, Brodmann areas and anatomical segmentation. DSI Studio uses linear

transformation to register Talairach atlas on subject's diffusion space. The Talairach coordinate system provides anatomical and functional information (Nowinski 2005). For comparison, FreeSurfer (<http://surfer.nmr.mgh.harvard.edu>) was used to automatically segment cortical gyral ROIs based on previous brain atlases (Desikan et al. 2006) using each participant's T_1 -weighted MPRAGE image.

Fiber Dissection Technique

Four normal brains (age 32–81 years, 3 females) were obtained at routine autopsy. The study was approved by CORID at University of Pittsburgh. The specimens were fixed in a 10% formalin aqueous solution for at least 4 weeks and then they were subsequently frozen for 2 additional weeks at -16°C , according to the method introduced by Ludwig and Klingler (1956; Agrawal et al. 2011) and used in multiple studies before (Türe et al. 2000; Choi et al. 2006; Fernández-Miranda, Rhoton, Alvarez-Linera et al. 2008; Fernández-Miranda, Rhoton, Kakizawa et al. 2008; Fernandez-Miranda et al. 2012). Progressive dissection of the white matter tracts was performed by peeling off the gray matter and isolating the fiber bundles in their glial sheets. We undertook the fiber dissection studies at the Surgical Neuroanatomy Lab (University of Pittsburgh) with the aid of microsurgical instrumentation and surgical microscope (6–40 magnification, Carl Zeiss, OPMI CS-NC).

Results

The Trajectory of the MdLF in the Human Brain

"Subject-Specific" Tractography Findings

Selective seeding along the superior temporal gyrus (Fig. 1A–C) consistently shows a large bundle of fibers that projects posterosuperiorly toward the parietal region (Fig. 1D–F). This distinct group of fibers originates from the anterior, middle, and posterior portions of the superior temporal gyrus (including the transverse temporal gyrus); they form a compact fascicle at the temporoparietal junction; and then they fan out as they approach the parietal region (Fig. 1C). In coronal and axial views, it can be clearly noticed that the MdLF makes a wide-angle turn at the temporoparietal junction that redirects the trajectory of the fibers from anterolateral (temporal region) to posteromedial (parietal region) (Fig. 1E,F).

"Template" Tractography Findings

The DSI template (NTU-90) showed similar results to the subject-specific tractography analysis (Fig. 2).

Fiber Dissection Findings

Microdissection is started at the lateral surface of the brain. The arcuate fascicle is the most lateral fiber tract and therefore the first to be encountered. It originates from the frontal region (inferior and middle frontal gyri), arches around the posterior margin of the insula, and terminates at the posterior temporal region (superior, middle, and inferior temporal gyri). Next, the temporal portion of the arcuate fascicle is removed to expose the temporoparietal junction located just posterior to the insula and deep to the arcuate fascicle. Starting at the superior temporal gyrus, there are large bundles of fibers originating from here that course posteriorly and upward beneath the previously removed arcuate fasciculus and toward the parietal region (Fig. 3A). This group of fibers forms the MdLF, and its trajectory is similar to that previously traced with the fiber tractography analysis (Fig. 3B). Removal of the superficial fibers of the MdLF reveals the presence of a deeper layer of fibers that also forms part of the stem of the

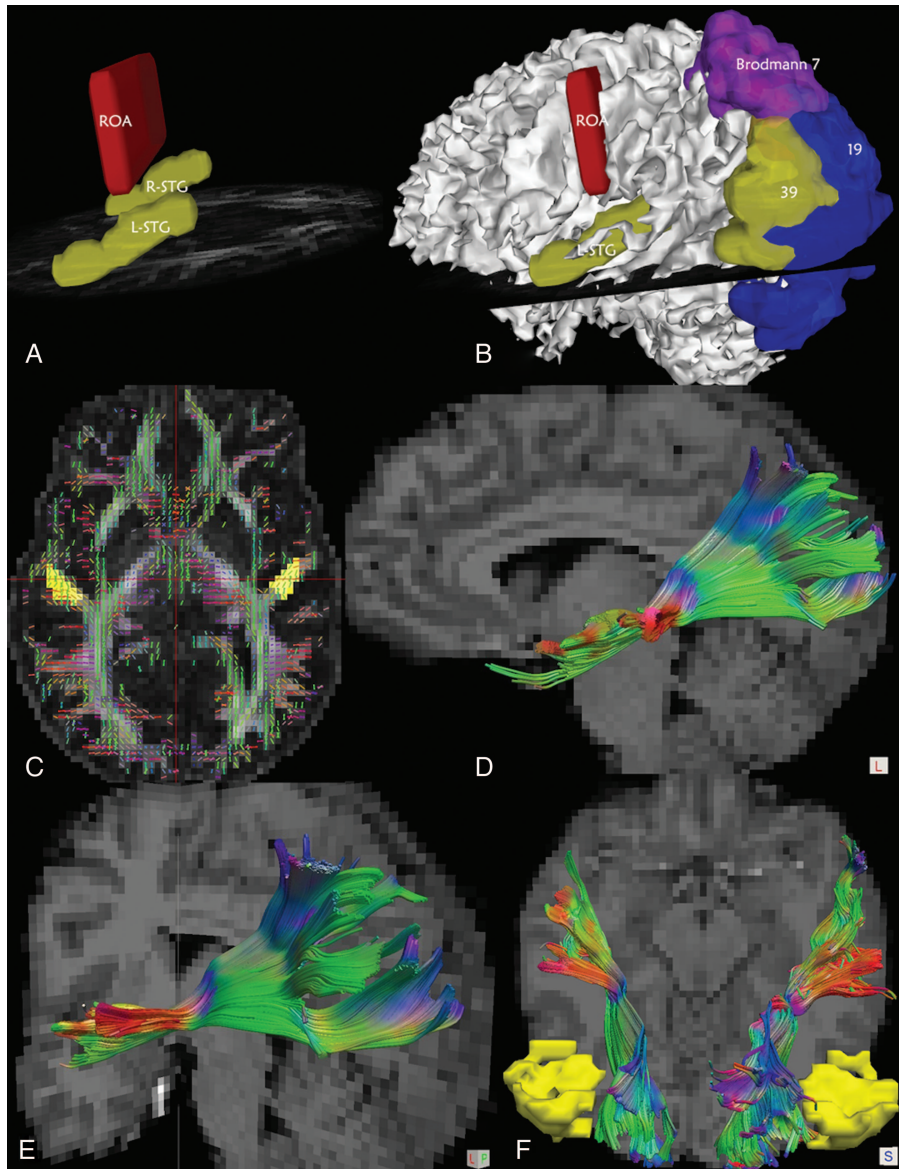


Figure 1. In vivo fiber tractography of the MdLF (subject-specific approach; subject number 5). (A) Seeding ROI and precentral ROA mask. (B) ROIs overlaid on white matter surface. (C) Axial slice at the midinsular level. Knowledge-based seeds at the superior temporal gyrus have been placed bilaterally (yellow areas). (D) Sagittal plane; lateral view of the left MdLF. (E) Combined coronal and sagittal view; the left MdLF runs from the superior temporal gyrus to the superior parietal lobule and parietooccipital region. (F) Axial plane; the left and right MdLF can be identified and both have similar trajectories.

MdLF. Interestingly, this deeper layer of fibers originates more anteriorly in the superior temporal gyrus, suggesting a characteristic segmentation pattern in the MdLF (Fig. 3*B–D*). The fibers of the MdLF are adjacent and immediately superficial to the fibers of the external capsule, specifically the dorsal external capsule (claustralcortical fibers) and ventral external capsule (inferior frontooccipital fascicle, IFOF). Please see Figure 4 and Supplementary Figs. 1 and 2 for a step-by-step and 3D version of the fiber microdissection of the MdLF.

The Spatial Relationship of the MdLF with Adjacent Association Tracts

Our results using in vivo fiber tractography and ex vivo fiber microdissection show the intimate anatomical relation of the MdLF with the arcuate, inferior occipitofrontal, dorsal external

capsule, and inferior longitudinal fascicles. The arcuate fascicle, as previously mentioned, is situated superficial to the MdLF; in particular, the arched portion of the arcuate fascicle covers the MdLF at the temporoparietal junction. Importantly, the arcuate fascicle mainly terminates at the superior, middle, and inferior temporal gyrus, while the MdLF terminates entirely at the superior temporal gyrus. The connections of the arcuate fascicle with the superior temporal gyrus are located just superficial to the terminations of the MdLF (Figs. 4 and 5) (Supplementary Figs. 1 and 2).

The IFOF is a large bundle of fibers that passes from the prefrontal region to the occipital region via the ventral part of the extreme and external capsules (Fernández-Miranda, Rhonot, Alvarez-Linera et al. 2008). This fascicle has been described in classic and contemporary neuroanatomical human studies (Türe et al. 2000; Catani et al. 2002; Fernández-

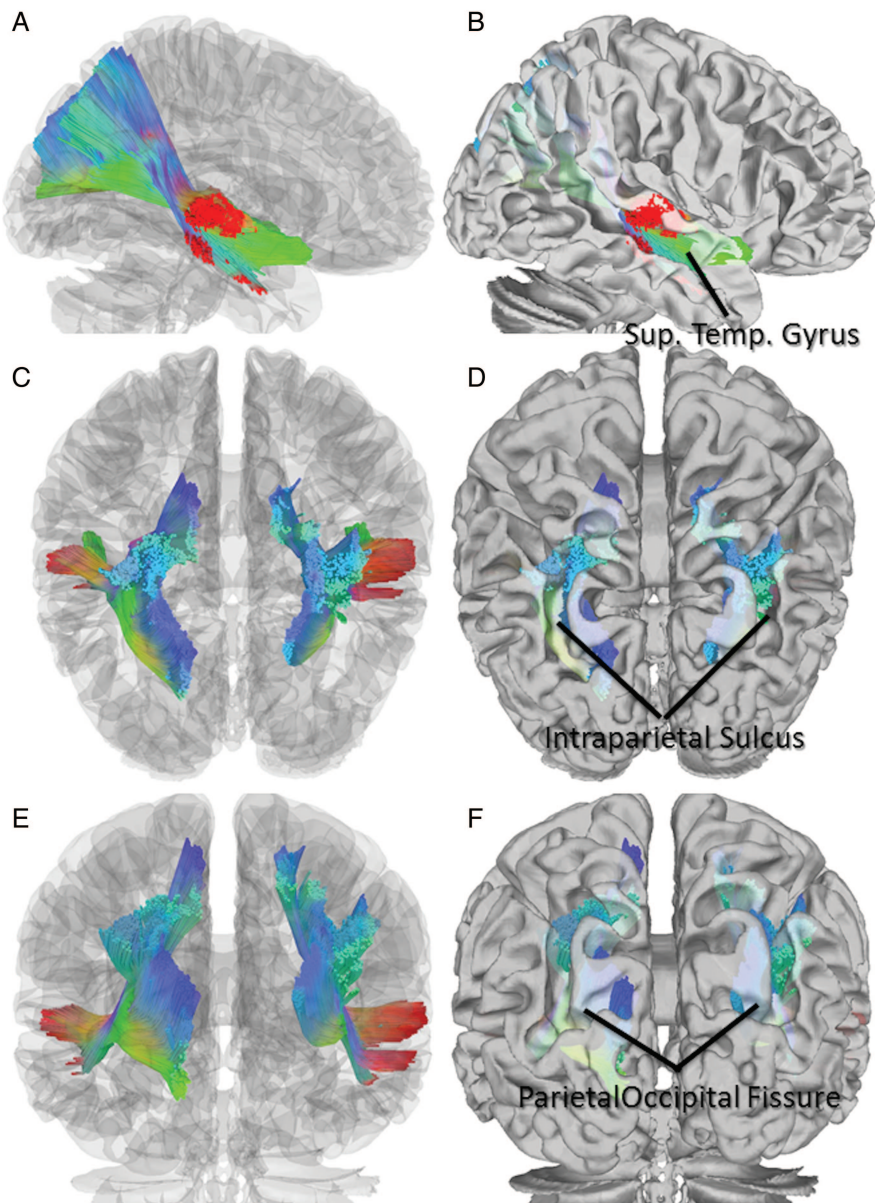


Figure 2. In vivo fiber tractography of the MdLF [DSI template; NTU90 Atlas (Yeh and Tseng 2011)]. The MdLF has been segmented following same strategy; sagittal (A and B), axial (C and D), and coronal (E and F) slices show the trajectory of the left and right MdLF on the NTU-90 Atlas, which represents the average of 90 DSI studies.

Miranda, Rhoton, Kakizawa et al. 2008; Martino et al. 2010), but recently, its existence in the human brain has been disputed based on the results of histological studies in animals (Schmahmann and Pandya 2006). To solve this controversy, we have recently proposed that the so-called extreme capsule in nonhuman primates' studies is the equivalent of the IFOF in humans (Fernandez-Miranda et al. 2010). Our fiber dissection studies show that adequate exposure of the IFOF requires complete removal of the superior temporal gyrus and MdLF (Supplementary Figs. 1 and 2). Therefore, the fibers of the IFOF at the posterior temporal region travel deep to the fibers of the MdLF, and they terminate at the cuneus in a more inferior location (closer to the calcarine fissure) than the MdLF terminations. The in vivo tractography reconstruction of the IFOF and MdLF demonstrates their intimate anatomical relationship and their distinct (but adjacent) termination fields in the parietooccipital region (Fig. 5).

The inferior longitudinal fasciculus (ILF) is an associative tract with long and short fibers connecting the occipital and temporal lobes (Catani et al. 2003) (Wakana et al. 2007). It travels within the white matter of the fusiform or occipitotemporal gyrus (Fernández-Miranda, Rhoton, Kakizawa et al. 2008). The in vivo tractography reconstruction of the ILF and MdLF showed that the ILF has a trajectory that is inferior to the MdLF running in close proximity and nearly parallel to the fibers of the MdLF (Fig. 5C).

Brain Connectivity of the MdLF

To demonstrate the connectivity of the MdLF, we investigate the terminal endpoints of the MdLF into the brain cortical surface on each subject's hemisphere (Fig. 5). Remarkably, the fiber tracking presented here accurately displays the cortical endpoints of the fiber tracts. At the superior temporal gyrus, the termination of the MdLF is mainly at Brodmann

area 22 (in 12 of 12 hemispheres), while the most anterior part of MdLF also terminates at Brodmann area 38 (in 10 of 12 hemispheres). The fibers of the MdLF run posteriorly and upward, and mainly terminate at Brodmann area 7 (located in the superior parietal lobe or precuneus) in all hemispheres; importantly, the most posterior and inferior portion of the MdLF also terminates at Brodmann area 19, which belongs to the parietooccipital region or cuneus, in 10 of 12 hemispheres. Only 1 of 12 hemispheres presented fiber terminations at Brodmann area 39, which encompasses the angular gyrus (Fig. 6) (Table 1). The analysis of the endpoints on the NTU-90 template showed similar results, with fibers terminating at areas 22, 38, 7, and 19 in both hemispheres (Fig. 2) (Table 1).

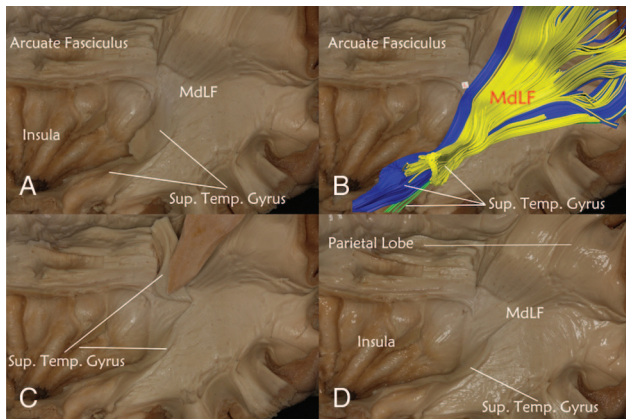


Figure 3. Fiber microdissection of the MdLF (left hemisphere, brain 1). (A) A large bundle of fibers originates from the superior temporal gyrus and courses posteriorly and upward toward the parietal region. (B) In order to facilitate identification of the fibers by the reader, the MdLF obtained with fiber tractography (subject 5, see Fig. 1) has been overlaid on the fiber dissection specimen. (C) The superficial layer of the MdLF is being removed. (D) After removal of the superficial layer of the MdLF the deep layer becomes evident.

Also, we completed the analysis of the cortical termination of the MdLF fibers by means of anatomical cortical parcellation (Desikan et al. 2006). We focused our investigation on the termination of the fibers at the parietal and occipital regions, and we identified two major cortical termination areas: superior parietal and occipital (superior and middle); both areas correspond to Brodmann areas 7 and 19, respectively. Considering all the hemispheres together, we found that 55% of the MdLF fibers were connecting with the superior parietal lobule and 40% with the occipital region (occipital superior and middle). In 6 of 12 hemispheres, we found a few fibers (from 0.4 to 10% of the total tract fibers) connecting with the angular gyrus of the inferior parietal lobule. Considering all the hemispheres together, the termination of the MdLF fibers at the angular gyrus represents only 5% of the total (Table 2). When analyzing in more detail the termination of the fibers at the angular gyrus, it appears than these fibers are located at the sulci level (intraparietal) and most medial portion of the angular gyrus, adjacent to the occipital region (Supplementary Fig. 3). The analysis of the DSI template revealed similar results, with most fibers connecting with the superior parietal and parietooccipital region, and just 7% of the MdLF fibers terminating at the angular gyrus (Table 2).

Qualitative and Quantitative Study of the MdLF: Intra and Intersubject Comparison

The results of our subject-specific fiber tractography study show that left and right MdLF have similar location, shape, and trajectory in all 12 hemispheres (Fig. 7). Furthermore, detailed analysis of the endpoints reveals no major intrasubject or intersubject difference in the cortical regions of termination: the MdLF consistently interconnects the superior temporal gyrus with the superior parietal lobule and superior occipital region, with minor and nonconstant connections with the angular gyrus. The mean total volume of the MdLF is 16.5 ± 2.5 mL with no significant difference between left and right hemispheres, or between subjects. The mean relative

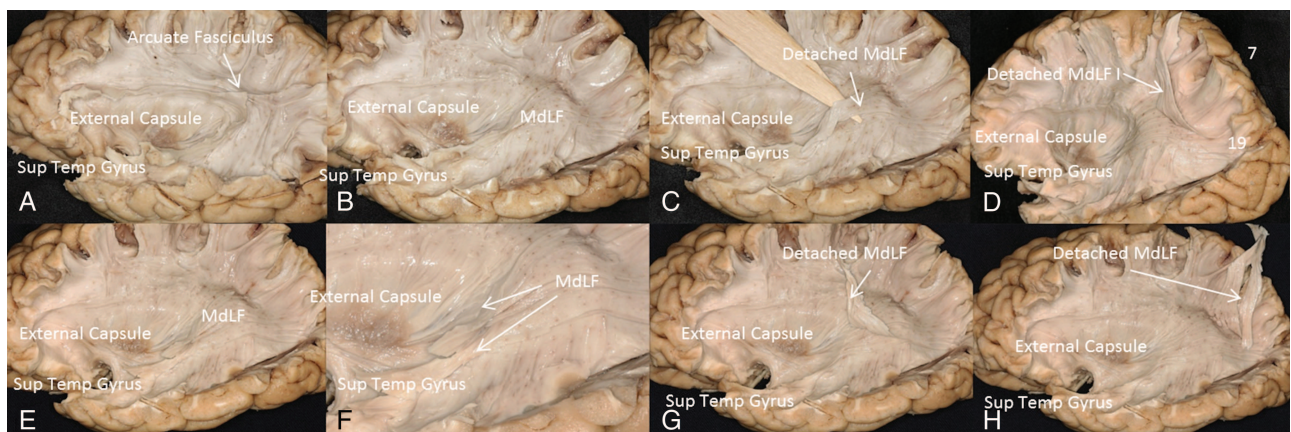


Figure 4. Step-by-step fiber microdissection of the MdLF (left hemisphere, brain 2). (A) The AF and external capsule have been exposed. (B) After complete removal of the AF we exposed the fibers of the MdLF running at the temporoparietal junction; the cortex of the superior temporal gyrus has been removed to better identify the underlying white matter fibers. (C and D) The fibers located within the superior temporal gyrus (origin of the MdLF) are detached and followed toward their destination at the superior parietal lobule and parietooccipital region. (E) The previously detached fibers of the MdLF are now repositioned to better appreciate their origin, trajectory, and spatial relationship with adjacent fiber tracts, such as the dorsal external capsule (claustral-cortical fibers) and ventral external capsule (IFOF). (F) Close-up view of (E). (G and H) The fibers originating at the superior temporal gyrus are further detached and followed toward their destination at the superior parietal lobule and parietooccipital region. The MdLF lies immediately superficial to the fibers of the external capsule.

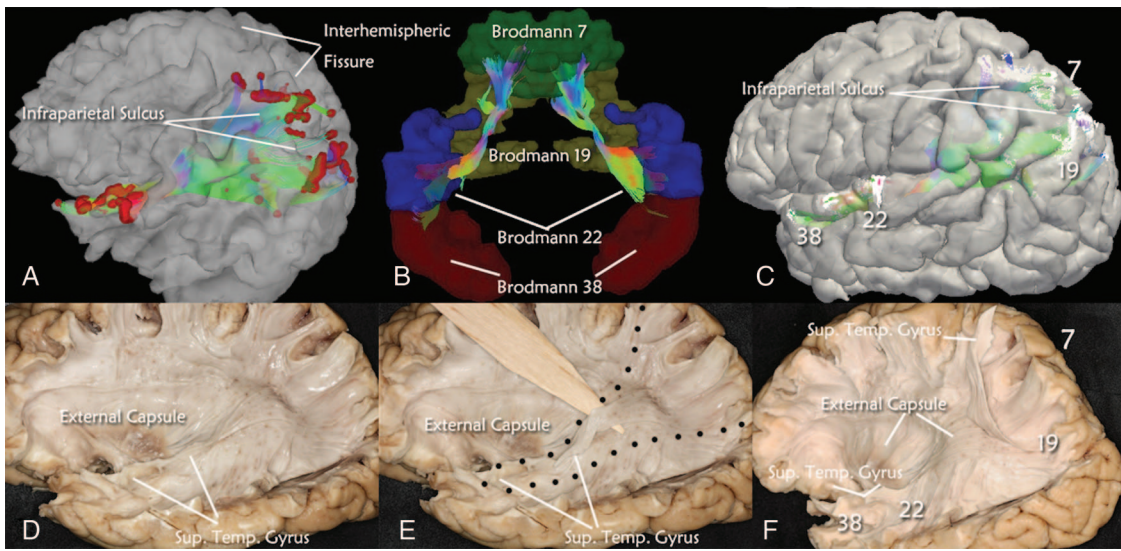


Figure 5. Cortical connectivity of the MdLF and its segmentation. (A) Left sagittal view; the origin and termination points (red areas) of the MdLF are displayed on the whole-brain surface. (B) Posterior coronal view; the MdLF originates mainly from Brodmann area 22 and terminates at Brodmann area 7, while some fibers also originate from Brodmann area 38 and terminate at area 19. (C) Sagittal view; overlay with T_1 freesurfer anatomical surface indicates that the MdLF interconnects the superior temporal gyrus (areas 38 and 22) with the superior parietal lobule and parietooccipital region (areas 7 and 19). (D and E) Fiber microdissection, to correlate with A–C. D, the white matter of the superior temporal gyrus has been dissected and isolated from the underlying external capsule fibers. (E) The posteriormost fibers of the superior temporal gyrus are being elevated and followed to their cortical destination in the superior parietal lobule and parietooccipital region; the approximate limits of the MdLF have been marked with black pins to facilitate identification. (F) The external capsule fibers can be recognized after dissection and elevation of the MdLF; Brodmann areas 7, 19, 22, and 39 have been localized to facilitate correlation with Figure 3C.

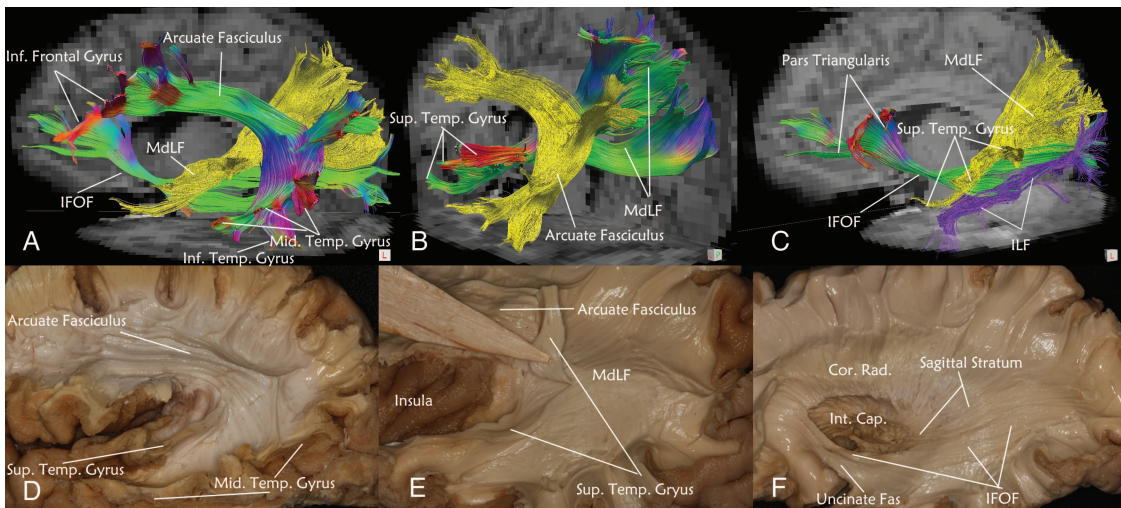


Figure 6. Spatial relationship of the MdLF with adjacent association tracts. (A) Sagittal view; the arcuate fascicle (RGB color) interconnects prefrontal and posterior temporal regions and has multiple fiber terminations at the inferior and middle temporal gyri. The MdLF (yellow) travels deep to the arcuate fascicle at the temporoparietal region. The IFOF (RGB color) runs deep to the MdLF at the posterior temporal regions. (B) Coronal view; the arcuate fascicle (yellow) is superficial to the MdLF (RGB color). (C) Sagittal view; the MdLF (yellow) is superficial to the IFOF (RGB color), and just superior to the ILF (purple). (D and E) Fiber microdissection, to correlate with A–C. D, arcuate fascicle. E, arcuate fascicle and MdLF. F, IFOF.

volume of the MdLF in relation to whole-brain volume is approximately 5.5%. The mean length of the MdLF is 90 ± 21 mm with no significant difference between left and right hemispheres or between subjects. The analysis of the NTU-90 template revealed similar results (Table 1).

Discussion

In this study, we present the trajectory, cortical connectivity, and descriptive analysis of the MdLF in 6 subjects and a template of 90 subjects. A prior report showed the trajectory and

connections of the human MdLF employing DTI MR-based technique (Makris et al. 2009). Here, we demonstrate a more complete connectivity pattern than previously stated that supports a different functional role of the MdLF in humans. Furthermore, we illustrate that extrapolation of data from white matter injection tracer studies in nonhuman primates may mislead our current understanding on human white matter anatomy and function.

Makris et al. (2009) completed the only study that has exclusively investigated the existence of the MdLF in the human brain. Employing DTI in 4 subjects, they described that the

Table 1

Quantitative study of the MdLF

MdLF	Side	S1	S2	S3	S4	S5	S6	NTU-90
Endpoints (Brodmann area)	L-parietal	7	7,19	7,19	7,19	7,19	7,19	7,19
	L-temporal	22,38	22,38	22	22,38	22,38	22,38	22,38
	R-parietal	7	7,19	7,19	7,19	7,19	7,19	7,19
	R-temporal	22	22,38	22,38	22,38	22,38	22,38	22,38
Volume (ml)	L	13.14	15.9	12.5	17.4	18	16	15.7
	R	15	21.8	14.9	18	17	18	17
Length (mm)	L	89 ± 13	89 ± 20	94 ± 8	92 ± 10	90 ± 8	90 ± 8	99 ± 12
	R	92 ± 12	81 ± 18	88 ± 12	96 ± 15	92 ± 7	92 ± 12	95 ± 17

Note: L, left; R, right; S, subject.

Table 2

Cortical anatomical parcellation of the MdLF

MdLF	Parietal inferior—angular (%)	Parietal superior (%)	Occipital (Sup, Mid) (%)
Subject 1	10 (right)	90	0
Subject 2	7.4 (left)	64.3	28.3
Subject 3	0	50	50
Subject 4	0.4 (right)	30	69.6
Subject 5	2 (bilateral)	51	47
Subject 6	10 (right)	46	44
Total	4.96	55.16	39.8
DSI template (NTU-90)	7	43	50

human MdLF has similar corticocortical connectivity than the non-human primate MdLF; in particular, they concluded that the human MdLF interconnects the inferior parietal lobule (angular gyrus) and the superior temporal gyrus, and is equivalent to the MdLF in monkeys. The technical limitations of this study were directly addressed by the authors "... Considering the limitation of the DT-MRI tractographic technique to allow precisely the tracking of the origins and terminations of fiber bundles, cortical parcellation presents the advantage to complement DT-MRI tractography in approximating the cortical regions of origin and termination of corticocortical association fiber tracts. Moreover, extrapolation from the experimental data in monkeys regarding the origins and terminations of fiber pathways provide additional information regarding the origin and terminations of a fiber bundle." Thus, the results of their study are based on the combination of cortical parcellation, which approximates cortical regions of termination, and extrapolation of "a priori" knowledge obtained from animal studies.

The results of our study are based on the combination of high-angular-resolution diffusion imaging, which allows direct investigation of the cortical termination of long-range fiber tracts, and human fiber microdissection, which provides insight into the stem and trajectory of major human fiber tracts. The form of diffusion imaging that we used (diffusion spectrum imaging; DSI) involves a dense sampling of angular space for underlying water diffusion (Wedgeen et al. 2008). This significantly improves our ability to reconstruct complex fiber crossings and partial volume effect that typically impair DTI tractography of pathways such as the MdLF, arcuate fasciculus, IFOF, and dorsal external capsule. Single-shell methods such as DTI offer better signal-to-noise on voxelwise measures of white matter integrity such as fractional anisotropy. However, once a minimum voxel-level signal-to-noise is

achieved, tractography can resolve the spatial extent of the fiber pathway, particularly in core regions away from gray matter edges (Wedgeen et al. 2008). Partial voluming is a potential concern for differences in voxel sizes between the DSI data used in the present study and the DTI data used by Makris et al. 2009. However, a 0.4-mm difference on a pathway that (by our findings) spans centimeters of space, cannot be explained as an artifact of partial voluming in a subset of voxels.

By integrating DSI with improved reconstruction and deterministic tractography approaches (Yeh et al. 2010), we can acquire significantly better resolution of otherwise difficult to map fiber pathways (Verstynen et al. 2011; Yeh et al. 2011) (Fernandez-Miranda et al. 2012). Our diffusion imaging technique involves a 43 min and 257-direction scan, as compared with the 10 min and 7-direction scan used by Makris et al. (2009). This is a major difference in fiber-tracking resolution that explains the differences in our results.

On the basis of our results, we believe that previous DTI studies, including ours (Fernández-Miranda, Rhoton, Kakizawa et al. 2008), were unable to completely differentiate and isolate the MdLF from the immediately adjacent fiber tracts, such as the arcuate, the IFOF, and the dorsal external capsule. In fact, we think that the close spatial relationship of the MdLF with these fiber structures is the main root of the biases in DTI results. We believe that the typical extension of the arcuate fascicle toward the anterior and middle segments of the superior temporal gyrus, as shown in multiple DTI studies, truly represents a false continuation artifact secondary to the apposition of the MdLF and the arcuate fascicle at the temporoparietal junction (Catani et al. 2002) (Fernández-Miranda, Rhoton, Kakizawa et al. 2008). Importantly, the IFOF, which travels within the ventral portion of the external capsule, runs just deep to the MdLF toward the occipital region, passing under the angular gyrus at the temporoparietooccipital junction; and the dorsal portion of the external capsule (claustracortical projection fibers and striatal projection fibers) runs just deep to the MdLF at the temporoparietal junction (Fernández-Miranda, Rhoton, Alvarez-Linera et al. 2008; Fernández-Miranda, Rhoton, Kakizawa et al. 2008). Wedeen et al. (2008) demonstrated that DTI cannot directly image multiple fiber orientations within a single voxel, while DSI can successfully image complex distributions of intravoxel fiber orientation. We think this fundamental difference between DTI and DSI techniques explains why previous studies using DTI were not able to completely differentiate the connectivity pattern of the MdLF from overlying (arcuate) or underlying (IFOF, dorsal external capsule) fiber tracts.

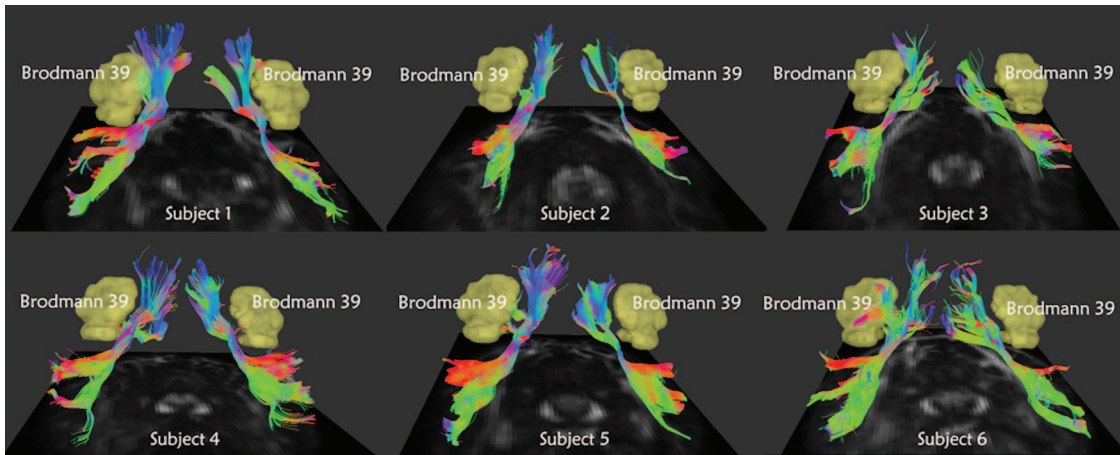


Figure 7. Qualitative study of the MdLF in 6 subjects and 12 hemispheres. Coronal view; note that the MdLF has similar intra and intersubject features. BA39 is lateral to the MdLF; only the right side of subject 6 has termination points at BA39.

A direct comparison of DTI and DSI datasets obtained in the same set of subjects would be needed to understand better the discrepancy between DTI and DSI studies in regards to the connectivity of the MdLF.

Remarkably, the connectivity pattern of the MdLF presented here was first obtained in 6 subjects (12 hemispheres), and then confirmed analyzing a DSI template of 90 subjects. The template approach does not allow for studying the individual differences as the subject-specific approach, but by averaging the data of a large sample it does provide unique information on the average connectivity patterns, and in this particular case, the average pattern of the MdLF. Importantly, both our subject-specific and template approaches show that the predominant connectivity of the superior temporal gyrus is with the superior parietal lobule and parietooccipital region, with minor connections to the angular gyrus. The absence of detecting another fiber tract connecting superior temporal gyrus and angular gyrus is a null result, and thus caution is warranted.

If we predefine the MdLF as the fiber tract that interconnects the superior temporal gyrus exclusively with the angular gyrus, as described by Makris et al. (2009), then only a minor (and nonconstant) group of fibers in our study would correspond to the MdLF, and the rest of fibers (superior temporal gyrus to superior parietal lobule and parietooccipital region) would correspond to a previously nondescribed temporoparietal fiber tract. However, we believe that the MDLF should be defined as the major fiber tract that interconnects the superior temporal gyrus with the parietal region, including the inferior and superior parietal lobules, and the parietooccipital region. Our study shows that the MdLF, defined as above, mainly connects the superior temporal gyrus with the superior parietal lobule and parietooccipital region, with additional nonconstant and minor connections with the inferior parietal lobule.

On the other hand, fiber dissection techniques were used by some of the early pioneers in human white matter anatomy to describe most fiber pathways in the human brain (Ludwig and Klingler 1956; Türe et al. 2000; Agrawal et al. 2011). Although lacking histological precision, fiber microdissection techniques are currently used to provide novel information on the anatomy of the fiber tracts at the macroscopic level. The combined application of fiber microdissection and fiber-tracking techniques for the study of human white matter

anatomy aids in proper interpretation and analysis of results (Fernández-Miranda, Rhiton, Alvarez-Linera et al. 2008; Fernández-Miranda, Rhiton, Kakizawa et al. 2008; Fernandez-Miranda et al. 2012). The two method cross-validation used here increases confidence in that the result is not an artifact of one method and provides stronger support for the described connectivity of the studied tract than either method alone.

Here, we show that the human MdLF differs from the monkey MdLF. Indeed, the human MdLF mostly interconnects the superior temporal gyrus with the superior parietal lobule and parietooccipital region, and not with the inferior parietal lobule, as previously stated (Schmahmann and Pandya 2006; Schmahmann et al. 2007; Makris et al. 2009). Remarkable differences between human and nonhuman primate white matter pathways have been recognized before (Rilling et al. 2008; Fernández-Miranda, Rhiton, Alvarez-Linera et al. 2008; Fernández-Miranda, Rhiton, Kakizawa et al. 2008). Rilling et al. (2008) compared the arcuate fascicle in macaques, chimpanzees, and humans, and concluded that the organization and cortical terminations of the arcuate fascicle were strongly modified in human evolution. In both humans and monkeys, the parietal cortex is separated by the intraparietal sulcus into a superior and an inferior lobule. The entire monkey inferior parietal lobule has been designated as Brodmann area 7; however, area 7 is the superior parietal lobule in the human brain. Several studies have indicated that Brodmann areas 7 in monkeys and humans are functionally homologous although anatomically different (Faugier-Grimaud et al. 1978; Lamotte and Acuña 1978; Jakobson et al. 1991; Karnath 2001). Consequently, it is logical from the evolutionary point of view that in monkeys the MdLF interconnects the superior temporal gyrus with the inferior parietal lobule, while in humans the MdLF does it with the superior parietal lobule.

The functional role of the human MdLF remains to be ascertained. In view of its connections, several authors have speculated that the MdLF plays a role in language (Schmahmann and Pandya 2006; Makris et al. 2009). Interestingly, a recent study involving awake craniotomy for brain tumor resection with subcortical electrostimulation demonstrated that no language interference is identified intraoperatively during electrostimulation and resection of the MdLF in the language dominant hemisphere. The authors found that no permanent language deficits are induced despite resection of a large part

of the MdLF, and postulated that the MdLF is not essential for language in humans (De Witt Hamer et al. 2011). Furthermore, the MdLF has no significant lateralization in fractional anisotropy or volume, as determined by a previous quantitative DTI study (Makris et al. 2009) and our study, respectively (see Table 1), while several structures that are essential for language display substantial asymmetry in concordance with language lateralization (De Witt Hamer et al. 2011).

From the results of our study, the MdLF does not primarily interconnect the superior temporal gyrus with the angular gyrus, but with the superior parietal lobule. The superior temporal gyrus, which contains Brodmann area 22, is involved in auditory processing. The superior parietal lobule, also known as posterior parietal cortex (Brodmann area 7), is involved in locating objects in space, serving as a multisensory processing center to determine where objects are in relation to parts of the body. Recently, Molholm et al. (2006) performed direct intracranial neurophysiology recordings from 3 human subjects and provided the first direct electrophysiological evidence for audio–visual multisensory processing in the human superior parietal lobule. Their study shows that auditory and visual sensory inputs project to the same highly localized region of the superior parietal lobule with auditory inputs arriving considerably earlier (30 ms) than visual inputs (75 ms). Here, we show the anatomic basis that explains such electrophysiological findings: the auditory inputs travel from the superior temporal region to the superior parietal lobule via the MdLF.

Based on our results and considering the role of the interconnected cortical regions, we hypothesize that the MdLF may constitute the “dorsal auditory pathway” or “where” pathway of the auditory system. More than 20 years ago, it was proposed that visual processing is divided into two essential functions: assigning meaning to an object (determining what it is), which was shown to occur in inferotemporal cortex, and accurately locating the object in space (determining where it is), which was found to occur in posterior parietal cortex (Ettlinger 1990; Lomber and Malhotra 2008; Farivar 2009). Multiple studies support the hypothesis that parallel cortical processing streams, similar to those identified in visual cortex, also exist in the auditory system (Lomber and Malhotra 2008). Over the last decade, a particularly prominent model of auditory cortical function proposes that a dorsal pathway, emanating from the posterior auditory cortex, is primarily concerned with processing the spatial features of sounds (Arnott and Alain 2011). Our results provide further support to the dual auditory stream model, and identify the MdLF as the potential pathway for the dorsal auditory stream. As opposed to a language-related tract, the dorsal auditory pathway would be part of a parallel transmodal neurocognitive network with no particular lateralization, explaining the absence of evident neurological deficits after its unilateral surgical resection or interruption (De Witt Hamer et al. 2011). Bilateral superior parietal lobule lesions such as in Balint’s syndrome, however, are characterized by significant deficits in both visual and auditory spatial localization (optic and auditory ataxia) (Phan et al. 2000). The investigation of the structural arrangement of the convergence of the auditory and visual dorsal pathways in the superior parietal lobule may help understanding the multisensory integration processes that give rise to the unified sensorial experience (Crick and Koch 2005).

Finally, the results presented here have several limitations. First, the subject-specific approach was completed in only 6 subjects; further studies with a larger number of subjects are needed to understand better the variability of the MdLF in the human brain. Second, the DSI template used in this investigation has a relatively low spatial resolution (3-mm isotropic resolution) in comparison to the resolution of current diffusion studies (2.4-mm isotropic resolution) and the desirable submillimetric resolution; the inadequate resolution may result in inaccurate mapping of the fine structures, and a better spatial resolution setting is needed to construct a high-definition brain atlas.

Supplementary Material

Supplementary material can be found at: <http://www.cercor.oxfordjournals.org/>.

Notes

Conflict of Interest: None declared.

References

- Agrawal A, Kapfhammer JP, Kress A, Wichters H, Deep A, Feindel W, Sonntag VK, Spetzler RF, Preul MC. 2011. Josef Klingler’s models of white matter tracts: influences on neuroanatomy, neurosurgery, and neuroimaging. *Neurosurgery*. 69:238–252.
- Alexander DC, Barker GJ. 2005. Optimal imaging parameters for fiber-orientation estimation in diffusion MRI. *Neuroimage*. 27:357–367.
- Arnott SR, Alain C. 2011. The auditory dorsal pathway: Orienting vision. *Neurosci Biobehav Rev*. 35:2162–2173.
- Basser PJ, Pajevic S, Pierpaoli C, Duda J, Aldroubi A. 2000. In vivo fiber tractography using DT-MRI data. *Magn Reson Med*. 44:625–632.
- Catani M, Howard RJ, Pajevic S, Jones DK. 2002. Virtual in vivo interactive dissection of white matter fasciculi in the human brain. *Neuroimage*. 17:77–94.
- Catani M, Jones DK, Donato R, Ffytche DH. 2003. Occipito-temporal connections in the human brain. *Brain*. 126:2093–2107.
- Choi C, Rubino P, Fernandez-Miranda JC, Rhiton AL, Jr. 2006. Meyer’s loop and the optic radiations in the Transsylvian approach to the mediobasal temporal lobe. *Neurosurgery*. 59:228–236.
- Crick FC, Koch C. 2005. What is the function of the claustrum? *Philos Trans R Soc Lond B Biol Sci*. 360:1271–1279.
- De Witt Hamer PC, Moritz-Gasser S, Gatignol P, Duffau H. 2011. Is the human left middle longitudinal fascicle essential for language? A brain electrostimulation study. *Hum Brain Mapp*. 32:962–973.
- Desikan RS, Ségonne F, Fischl B, Quinn BT, Dickerson BC, Blacker D, Buckner RL, Dale AM, Maguire RP, Hyman BT et al. 2006. An automated labeling system for subdividing the human cerebral cortex on MRI scans into gyral based regions of interest. *NeuroImage*. 31:968–980.
- Ettlinger G. 1990. “Object vision” and “spatial vision”: the neuropsychological evidence for the distinction. *Cortex*. 26:319–341.
- Farivar R. 2009. Dorsal-ventral integration in object recognition. *Brain Res Rev*. 61:144–153.
- Faugier-Grimaud S, Frenois C, Stein DG. 1978. Effects of posterior parietal lesions on visually guided behavior in monkeys. *Neuropsychologia*. 16:151–168.
- Fernandez-Miranda JC, Pathak S, Engh J, Jarbo K, Verstynen T, Yeh FC, Wang Y, Mintz A, Boada F, Schneider W et al. 2012. High-definition fiber tractography of the human brain: neuroanatomical validation and neurosurgical applications. *Neurosurgery*. 71:430–453.
- Fernandez-Miranda JC, Pathak S, Schneider W. 2010. High-definition fiber tractography and language. *J Neurosurg*. 113:156–157.

- Fernández-Miranda JC, Rhoton AL, Jr, Alvarez-Linera J, Kakizawa Y, Choi C, de Oliveira EP. 2008. Three-dimensional microsurgical and tractographic anatomy of the white matter of the human brain. *Neurosurgery*. 62:989–1026.
- Fernández-Miranda JC, Rhoton AL, Jr, Kakizawa Y, Choi C, Alvarez-Linera J. 2008. The claustrum and its projection system in the human brain: a microsurgical and tractographic anatomical study. *J Neurosurg*. 108:764–774.
- Fonov V, Evans AC, Botteron K, Almli CR, McKinstry RC, Collins DL. 2011. Unbiased average age-appropriate atlases for pediatric studies. *Neuroimage*. 54:313–327.
- Jacobson LS, Archibald YM, Carey DP, Goodale MA. 1991. A kinematic analysis of reaching and grasping movements in a patient recovering from optic ataxia. *Neuropsychologia*. 29:803–809.
- Karnath HO. 2001. New insights into the functions of the superior temporal cortex. *Nat Rev Neurosci*. 2:568–576.
- Lamotte RH, Acuña C. 1978. Defects in accuracy of reaching after removal of posterior parietal cortex in monkeys. *Brain Res*. 139:309–326.
- Lomber SG, Malhotra S. 2008. Double dissociation of ‘what’ and ‘where’ processing in auditory cortex. *Nat Neurosci*. 11:609–616.
- Ludwig E, Klingler J. 1956. *Atlas cerebri humani: the inner structure of the brain demonstrated on the basis of macroscopical preparations*. Boston: Little, Brown.
- Makris N, Papadimitriou GM, Kaiser JR, Sorg S, Kennedy DN, Pandya DN. 2009. Delineation of the middle longitudinal fascicle in humans: a quantitative, *in vivo*, DT-MRI study. *Cereb Cortex*. 19:777–785.
- Martino J, Brogna C, Robles SG, Vergani F, Duffau H. 2010. Anatomic dissection of the inferior fronto-occipital fasciculus revisited in the lights of brain stimulation data. *Cortex*. 46(5):691–699.
- Molholm S, Sehatpour P, Mehta AD, Shpaner M, Gomez-Ramirez M, Ortigue S, Dyke JP, Schwartz TH, Foxe JJ. 2006. Audio-visual multisensory integration in superior parietal lobule revealed by human intracranial recordings. *J Neurophysiol*. 96:721–729.
- Nowinski WL. 2005. The cerefy brain atlases: continuous enhancement of the electronic talairach-tournoux brain atlas. *Neuroinformatics*. 3:293–300.
- Phan ML, Schendel KL, Recanzone GH, Robertson LC. 2000. Auditory and visual spatial localization deficits following bilateral parietal lobe lesions in a patient with Balint’s syndrome. *J Cogn Neurosci*. 12:583–600.
- Rilling JK, Glasser MF, Preuss TM, Ma X, Zhao T, Hu X, Behrens TE. 2008. The evolution of the arcuate fasciculus revealed with comparative DTI. *Nat Neurosci*. 11:426–428.
- Schmahmann JD, Pandya DN. 2006. *Fiber pathways of the brain*. Oxford, New York: Oxford University Press.
- Schmahmann JD, Pandya DN, Wang R, Dai G, D’Arceuil HE, de Crespigny AJ, Wedeen VJ. 2007. Association fibre pathways of the brain: parallel observations from diffusion spectrum imaging and autoradiography. *Brain*. 130:630–653.
- Seltzer B, Pandya DN. 1984. Further observations on parieto-temporal connections in the rhesus monkey. *Exp Brain Res*. 55:301–312.
- Türe U, Yaşargil MG, Friedman AH, Al-Mefty O. 2000. Fiber dissection technique: lateral aspect of the brain. *Neurosurgery*. 47:417–426.
- Verstynen T, Jarbo K, Pathak S, Schneider W. 2011. In vivo mapping of microstructural somatotopies in the human corticospinal pathways. *J Neurophysiol*. 105:336–346.
- Wakana S, Caprihan A, Panzenboeck MM, Fallon JH, Perry M, Gollub RL, Hua K, Zhang J, Jiang H, Dubey P et al. 2007. Reproducibility of quantitative tractography methods applied to cerebral white matter. *Neuroimage*. 36:630–644.
- Wedgeen VJ, Wang RP, Schmahmann JD, Benner T, Tseng WY, Dai G, Pandya DN, Hagmann P, D’Arceuil H, de Crespigny AJ. 2008. Diffusion spectrum magnetic resonance imaging (DSI) tractography of crossing fibers. *Neuroimage*. 41:1267–1277.
- Yeh FC, Tseng WY. 2011. NTU-90: a high angular resolution brain atlas constructed by q-space diffeomorphic reconstruction. *Neuroimage*. 58:91–99.
- Yeh FC, Wedeen VJ, Tseng WY. 2011. Estimation of fiber orientation and spin density distribution by diffusion deconvolution. *Neuroimage*. 55:1054–1062.
- Yeh FC, Wedeen VJ, Tseng WY. 2010. Generalized q-sampling imaging. *IEEE Trans Med Imaging*. 29:1626–1635.